

Photochemical Oxidation on Nanorod Photocatalysts

Philip Kalisman¹, Yaron Kauffmann², and Lilac Amirav^{1*}

¹*Schulich Faculty of Chemistry, The Russell Berrie Nanotechnology Institute, and The Nancy and Stephen Grand Technion Energy Program; Technion – Israel Institute of Technology, Haifa 32000, Israel*

²*Department of Materials Engineering, Technion-Israel Institute of Technology, Haifa 32000, Israel*

Supplemental Information

Synthesis of Cadmium Selenide Quantum Dots (CdSe QDs)¹:

For the synthesis of CdSe QDs, 60mg cadmium oxide (CdO), 3g trioctylphosphine oxide (TOPO), and 280mg octadecylphosphonic acid (ODPA) were mixed in a three neck flask. The mixture was put under argon and heated to 150°C. At this point the solution was put under vacuum for 30min and then returned to Ar. The solution was heated to 370°C, at which point trioctylphosphine (TOP) was added to the clear solution. After the temperature recovered to the previous point a solution of TOP, and selenium was injected into the flask. After a set amount of time (0-5min depending on the desired size), the solution was removed from heat. Once cool, toluene was added to the solution which was cleaned by repeated precipitation by methanol and redissolution in toluene. The resultant solution was characterized by absorption spectroscopy for use in the growth of CdS@CdSe.

Synthesis of Cadmium Sulfide Seeded Rods (CdS@CdSe)^{2,3}:

For the synthesis of CdS@CdSe, CdO, TOPO, hexylphosphonic acid (HPA), and ODPA were mixed in a three neck flask (see table S1 for examples). The mixture was put under argon. After various heating/vacuum stages (depending on the method) a final temperature was reached (320-380°C, also depending on the method), at which point 1.5g TOP was added to the clear solution. After the temperature recovered to the previous point a mixture of 1.5g TOP, 120mg sulfur, and CdSe QDs were injected into the flask, and were left for eight or more minutes. The CdSe used for injection was collected by drying a desired volume of seeds, which were then redissolved in TOP. After a desired amount of time the solution was removed from heat. Once cool, toluene was added to the solution. The rods were cleaned by repeated redissolution in combinations of toluene, hexane, octylamine and nonanoic acid, and precipitated by centrifugation with methanol as the non-solvent. A final cleaning step was done in order remove short rods, seeds and tetrapods, using toluene, isopropanol and a centrifugation at 4000rpm for 30 minutes. Finally, the pellet was redissolved in toluene. Successful synthesis and cleaning resulted in uniform rods of high quality and quantity (Figure S1) which were used for further experimentation.

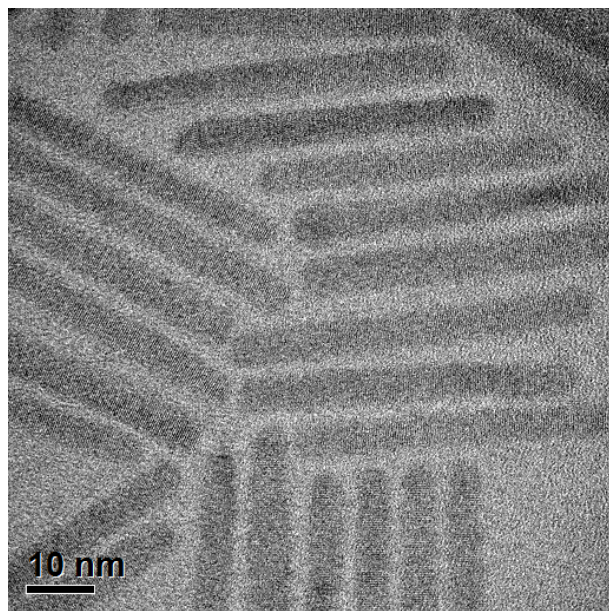


Figure S1. TEM micrograph of CdS@CdSe nanoparticles as grown

Resultant CdS@CdSe Length	32.7 ± 3.6	44.7 ± 3.1	50.4 ± 4.1
TOPO (g)	3.3	3	3
ODPA (g)	1.08	0.29	0.29
HPA (mg)	80	80	80
CdO (mg)	207	60	60
Seeds (uL) [diameter in nm] ^{4,5}	400 [3.0]	350 [2.5]	350 [2.5]
Reaction Temp (°C)	320	360	380
Reaction Time	10 min	8 min	15 min

Table S1. Typical precursor amounts and conditions for CdS@CdSe growth

Ligand Exchange:

CdS@CdSe rods were transferred from toluene to water by first precipitating the rods, using centrifugation with methanol as the non-solvent. The pellet was redissolved in a mixture of methanol, mercaptoundecanoic acid, and tetramethylammonium hydroxide. Once dissolved the rods were precipitated out using toluene as a non-solvent and further centrifugation. This pellet was then dissolved in water, methanol, or other polar solvent as desired.

Iridium Oxide Growth on the CdSe@CdS Rods:

Growth of iridium oxide was done by mixing variable amounts of precursors in a polystyrene cuvette. Typical solutions contained 5mg NaNO_3 , 3mg Na_3IrCl_6 , 9.5mg $\text{Na}_2\text{S}_2\text{O}_8$, and 16mg NaOH , plus seeded rods (in water) diluted to 2mL total with H_2O . The cuvette was capped and illuminated using either a Thorlabs 455-nm mounted LED or an Oriel arc lamp, with 300W Xenon source, for the desired amount of time. During illumination IrO_2 particles formed along the surface of the CdS@CdSe nanorods (Figure S2 and S3) and reactions that were not illuminated resulted in no such particles (Figure S4A). The solution was then transferred to a centrifuge tube and centrifuged at 7500rpm for 10-15minutes. The resultant pellet was dispersed in methanol or other polar solvent by brief sonication.

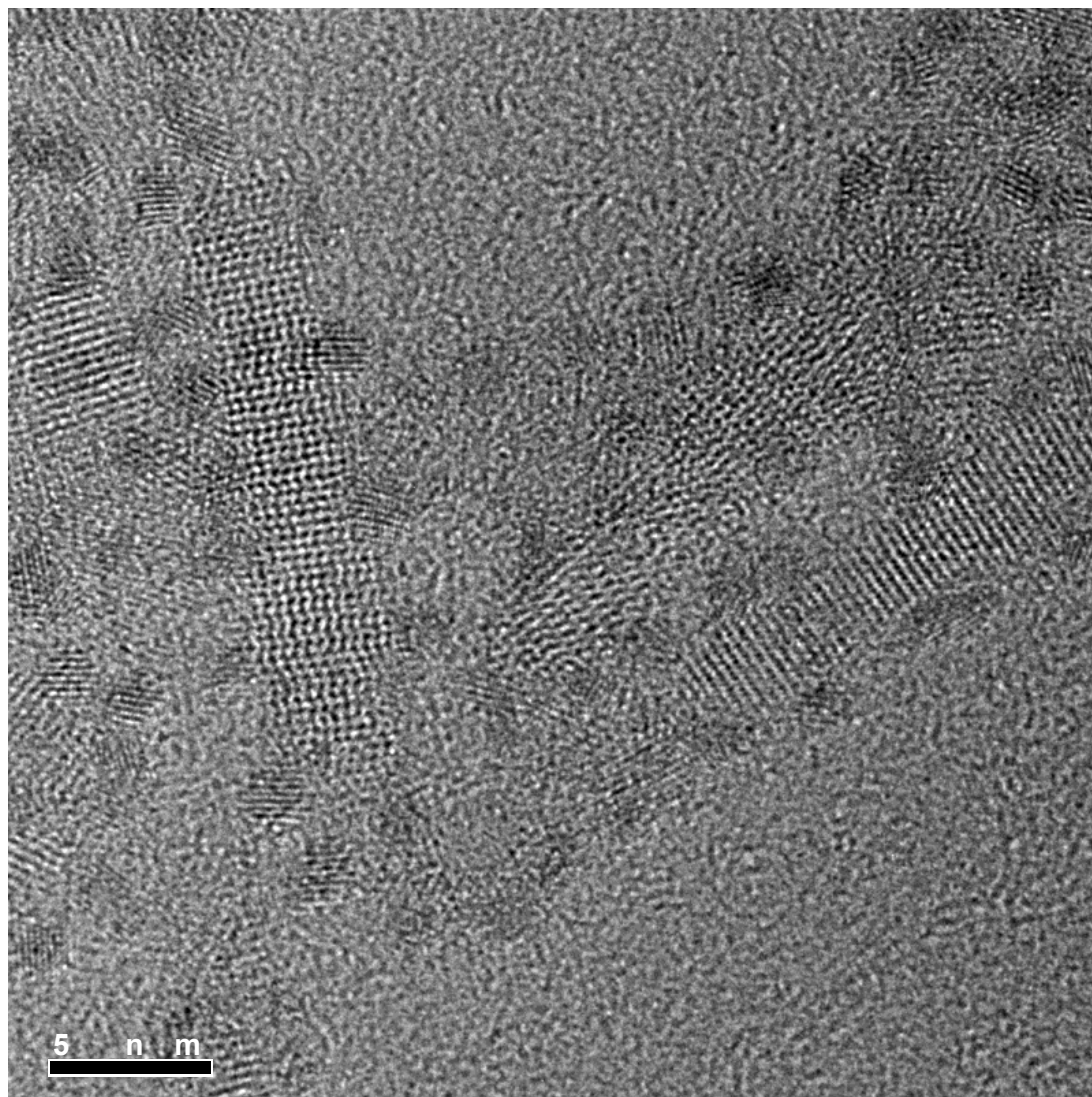


Figure S2. TEM micrograph of IrO_2 particles on CdS@CdSe nanorods

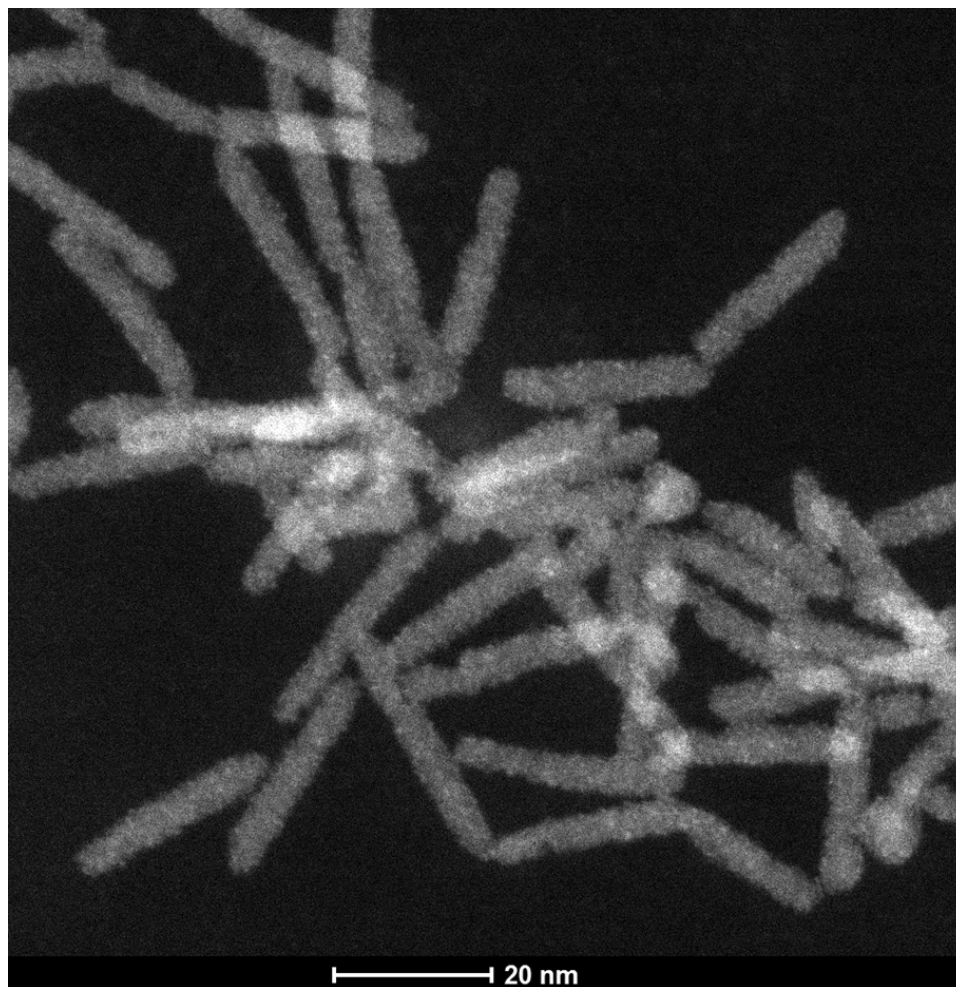


Figure S3. HAADF micrograph of CdS@CdSe nanorods (grey) covered in IrO₂ particles (white speckles)

The effects of various parameters on the growth of IrO₂ were investigated. Illumination intensities between 50-450mW were investigated, and found to have little impact on the growth rate or resultant particle size. This works well with our hypothesis that the growth is not done by a direct hole transfer, but mediated by oxidation of species within the solution. A direct hole attack would result not only with localized deposition of IrO₂ around the seed, but is also expected to demonstrate linear dependency on the illumination intensity. Thus, a moderate effect of illumination intensity can only be explained by a mediated oxidative pathway, where the overall reaction mechanism and kinetics are much more complex. Particle size was directly correlated with illumination time (Figure S4). Illumination for short periods of time resulted in coverage by small (0.5-1nm) IrO₂ particles, while longer illumination allowed for the

growth of particles of 2-3nm. If illumination was continued for long enough, the rods get completely coated in IrO₂ particles, making them appear about twice as thick as they are (Figure S4 E,F).

The effect of illumination wavelength was also examined. While generally the entire CdS rod was excited, we explored IrO₂ deposition under selective excitation of the CdSe seed. The IrO₂ nanoparticles appeared to be much smaller and after 6h of illumination resembled the particles that were obtained after only 45 min with the standard conditions.

The pH of the solution was controlled by adjusting the amount of NaOH used. The rate of particle growth appears to increase with an increase in pH, though this relationship has not been specifically calculated as the pH is typically above 13, making it difficult for us to accurately measure accurately, even with accurate measurement of NaOH. Because of this high pH, all glassware was avoided throughout the reaction in order to prevent dissolution or etching of silica into the solution. Besides controlling NaOH concentration, we also looked at the effect of NaNO₃ concentration on our growth product⁶, varying the NaNO₃ concentration from 0mM to 60mM. At low NaNO₃ concentrations metallic iridium can be grown along with the iridium oxide, however, the control of this selective growth has yet to be optimized. Various iridium precursors were also investigated; we were not able to grow any iridium particles using either ammonium hexachloroiridate or bis(1,5-cyclooctadiene)diiridium dichloride as the as iridium source.

Figure S4. TEM micrographs, showing the growth of IrO₂ particles over time. (A) Control, kept in the dark. The control shows no IrO₂ growth, and rods of approximately 4-5nm diameter, unchanged from before the experiment. (B-F) Samples illuminated with unfiltered lamb light for (B) 10 minutes, (C) 45 minutes, (D) 2 hr, (E-F) 4 hr. This series shows the progression from small ~0.5nm IrO₂ dots to larger particles with diameters of 2nm or more, to a full coating of IrO₂ particles The rods that were illuminated for 4 hours have a total diameter of 9-10nm, this increase in diameter matches a coating of IrO₂ that is 2-3nm thick

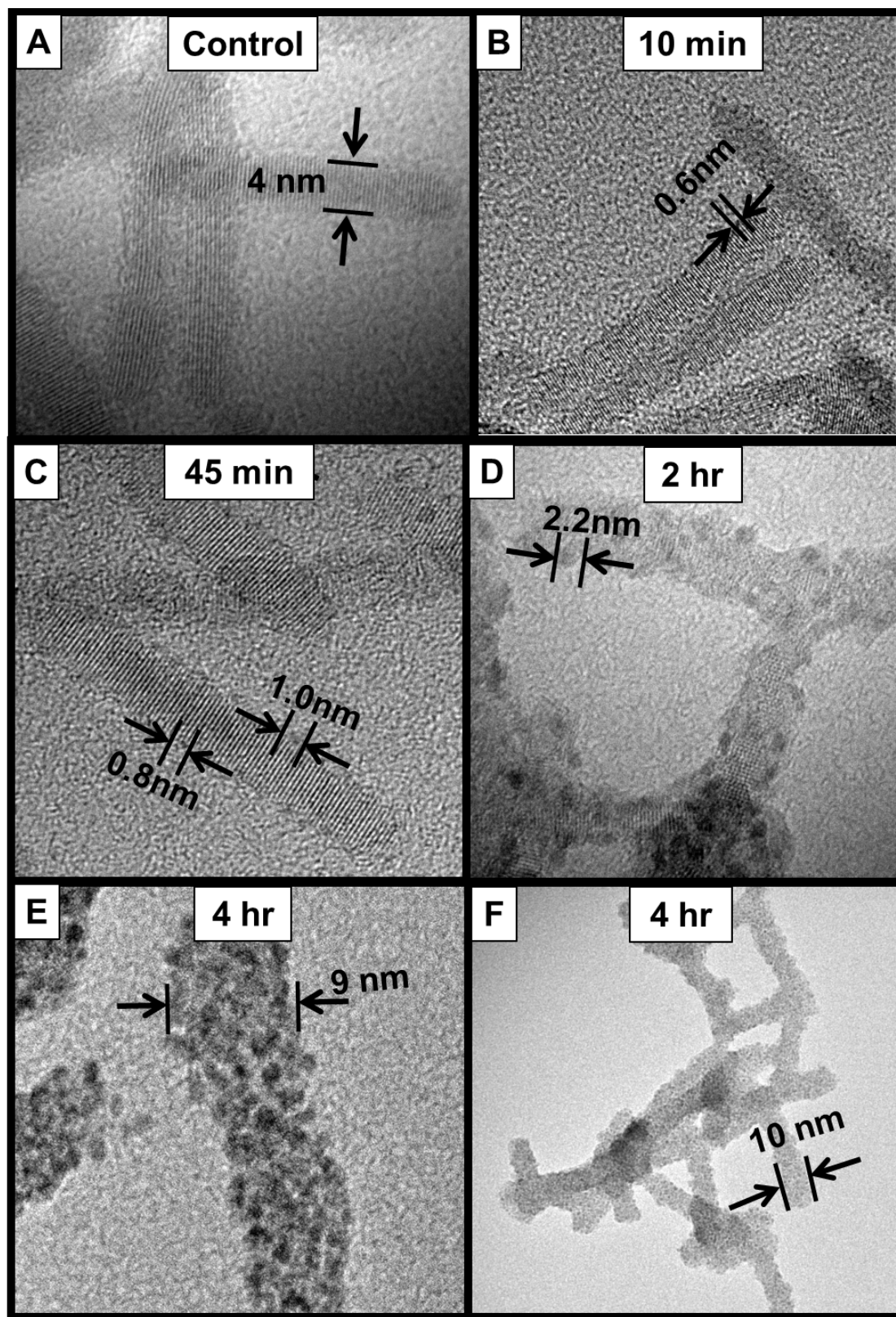


Figure S4. Caption above

Cobalt Oxide Growth:

Growth of cobalt oxide was done using a solution of cobalt acetoacetate, CdS@CdSe nanorods, dissolved in toluene, followed by the addition of perfluorodecaline. These solutions were made in glass cuvettes and illuminated similarly to solutions used in iridium oxide growth.

Characterization of Particles:

Transmission Electron Microscopy and Electron Dispersive Spectroscopy were done on a FEI Tecnai G² T20 S-Twin TEM, running at 200keV with a LaB₆ electron source and an FEI Supertwin Objective Lens or on a FEI Titan 80-300 KeV S/TEM at 300keV with a field emission gun electron source.

Samples for TEM were prepared by either dropping the solution directly or by aerosolized spray onto 300 mesh ultrathin carbon on lacey carbon grids purchased from Ted Pella Inc.

X-ray photoelectron spectroscopy (XPS) was done using a Thermo-VG SIGMA probe. Samples were prepared by drying solutions of particles suspended in water or methanol and allowed to dry on a glass slide or piece of a Si wafer. Deconvolution of signals was done using XPS-Peak Version 4.1. The whole signal was shifted based on the position of the C-1s peak, so that it was exactly 284.8eV. For analysis of Ir-4f peaks a Shirley background was subtracted, the LG% for the peaks was fixed at 30%, and the peak FWHM was constrained to 1.6-1.7; furthermore the FWHM for peak pairs was forced to be equal and the ratio of areas between the 4f_{5/2} to 4f_{7/2} was set to 3:4. Peak positions based on these deconvolutions were compared to literature values in order to identify the iridium state. Literature values vary greatly for peaks positions and spin orbit splitting energy reported for Ir(0), Ir(III), and Ir(IV)^{7,8,9,10}. The peak positions observed in our deconvoluted signal of 62.45eV/65.43eV and 64.08eV/67.06eV match closely to those reported by both *Hammond, et al*¹¹ (peak positions of 62.3eV/65.1eV and 63.2eV/66.5eV), and *Banerjee, et al*¹² (peak positions of 62.04eV/65.12eV and 63.7eV/66.42eV), each of which report a mixture of IrO₂ and Ir₂O₃. Similar analysis to that done for Ir-4f was done for the Ir-5d and O-1s peaks as well. The presence of Ir-5d peaks at 297.3eV and 313.1eV (figure 1) along with the bimodal hump of O-1s (figure 5S) further support that iridium oxide is present^{13,14,15}.

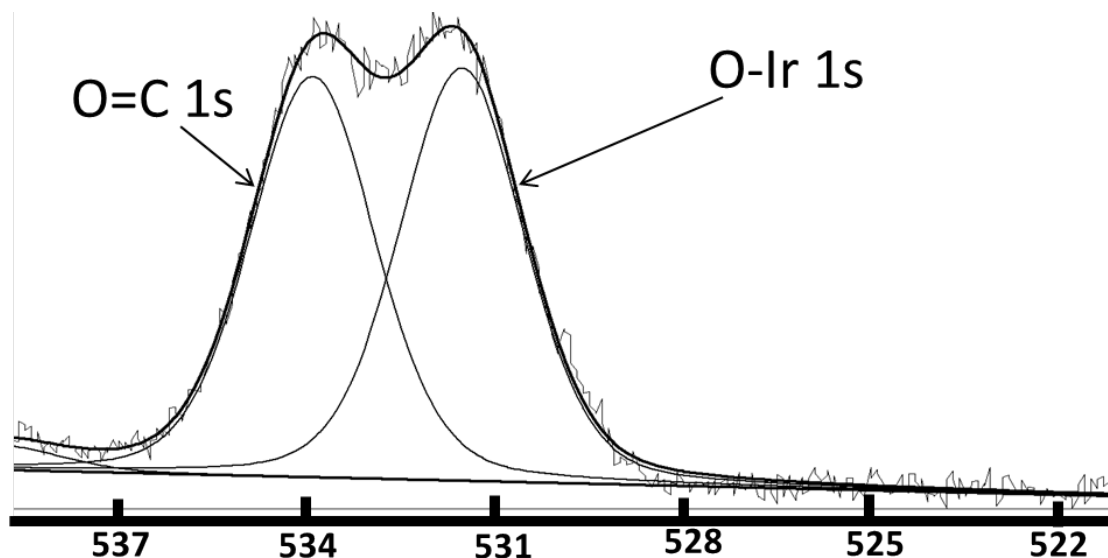


Figure S5. XPS of the region around the O-1s peak for a sample decorated with photochemically grown IrO_2 .

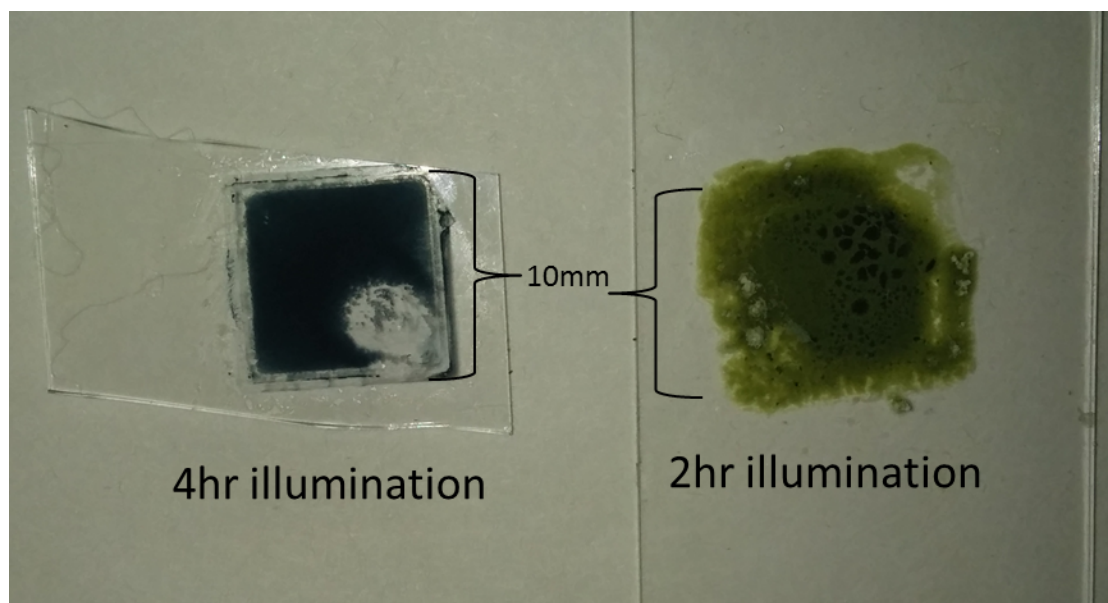


Figure S6. Photograph of samples prepared on glass slides, using the inverted cuvette method described below.

X-ray diffraction (XRD) spectroscopy was done using a Rigaku Miniflex X-ray Diffractometer. Samples were prepared by filling a cuvette with precipitated particles, covered the opening of the cuvette with a glass slide and then inverting the sample. The solvent was allowed to slowly evaporate off, leaving a 1cm x 1cm square of sample (figure S6). These samples were then analyzed using the Rigaku diffractometer. The collected signals were compared to JCPDS powder diffraction files in order to identify peaks.

Spectra taken after different illumination times showed a growing peak near $2\theta=23^\circ$, indicating time dependent growth of a crystalline material. High resolution spectra taken for clean rods, and rods after two hours of photochemical growth of iridium oxide were also taken (figure S8). Signal from the CdSe@CdS rod sample shows a match with the expected pattern for CdS [PDF# 00-006-0314], with missing peaks attributed to the preference for the clean rods to lay flat on the substrate. Signal from CdSe@CdS rods after growth of iridium oxide show the characteristic CdS peaks, along with extra peaks, including the one seen in figure S6. Some of these peaks match well with IrO₂ [PDF# 00-015-0870], while others match well with Rh₂O₃ [PDF# 01-076-0148] (which has been theorized to have a structure nearly identical to Ir₂O₃ - the pattern for Ir₂O₃ is not reported in the JCPDS database because it is relatively unstable)¹⁶. Similar to the XPS data, this XRD data confirms the presence of IrO₂, and suggests the iridium growth is a mix of IrO₂ and Ir₂O₃.

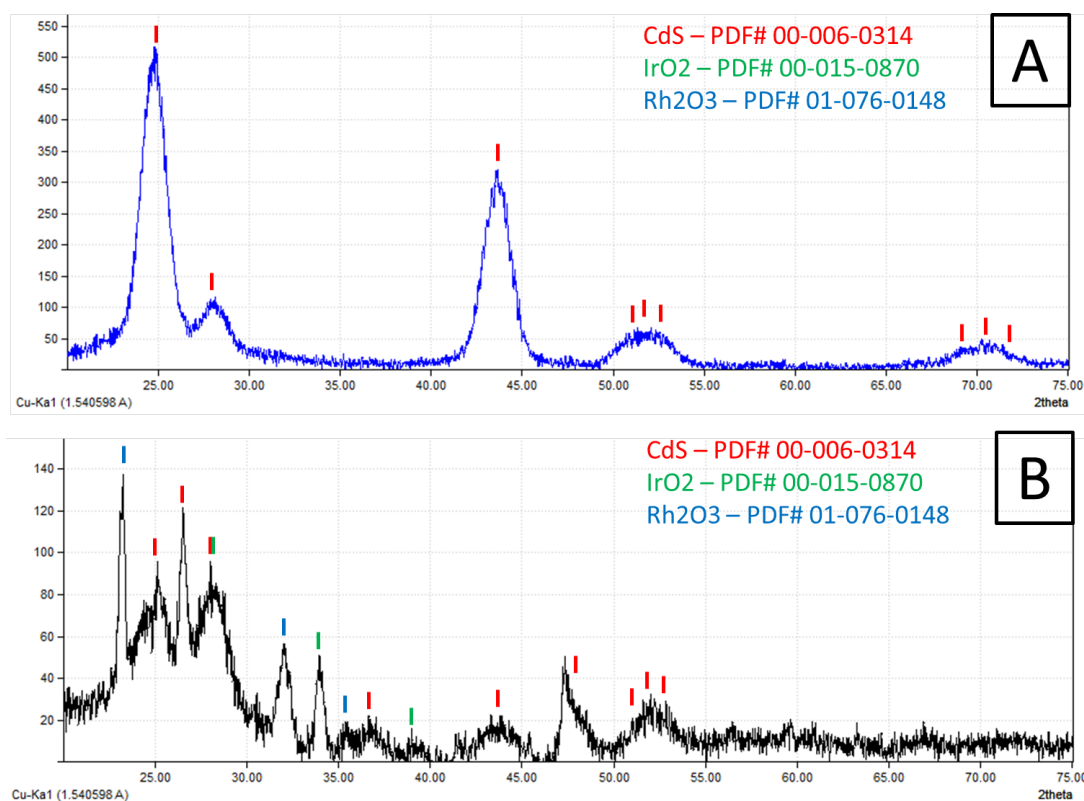


Figure S7. XRD pattern of a) plain CdSe@CdS rods b) CdSe@CdS rods coated with iridium oxide after 2hr illumination. The colored tick-marks above each pattern have been added to show assignments of peaks based on PDF cards.

Table S2. Peak positions for XRD patterns in figure S7 compared to PDF card values

Figure S8-A	Figure S8-B	CdS (00-006-0314)	IrO ₂ (00-015-0870)	Rh ₂ O ₃ (01-076-0148)
	23.4			23.94 (012)
24.7	25.1	24.82 (100)		
	26.6	26.45 (002)		
28.1	28.1	28.22 (101)	28.05 (110)	
	32.2			32.99 (104)
	34.0		34.71 (101)	
	35.5			35.22 (110)
	36.8	36.65 (102)		
	39.4		40.06 (200)	
43.7	43.6	43.74 (110)		
51.8	52.1	50.95 (103) 51.88 (112) 52.85 (201)		
70.2		69.37 (210) 70.96 (211) 72.47 (114)		

UV-Vis absorption spectroscopy was done using an Agilent Cary 5000 UV-Vis-NIR spectrophotometer using standard 10mm cuvettes. Spectra were studied using the accompanying Cary WinUV software package. Spectra were used frequently to determine seed size, seed concentration, rod concentration, as well as to study the photo-degradation of clean and coated rods. Further, CdS@CdSe was quickly identified by the presence of a strong shoulder near 475nm, corresponding to absorption by CdS, and a small peak due to the absorption of the embedded QD (Figure S9).

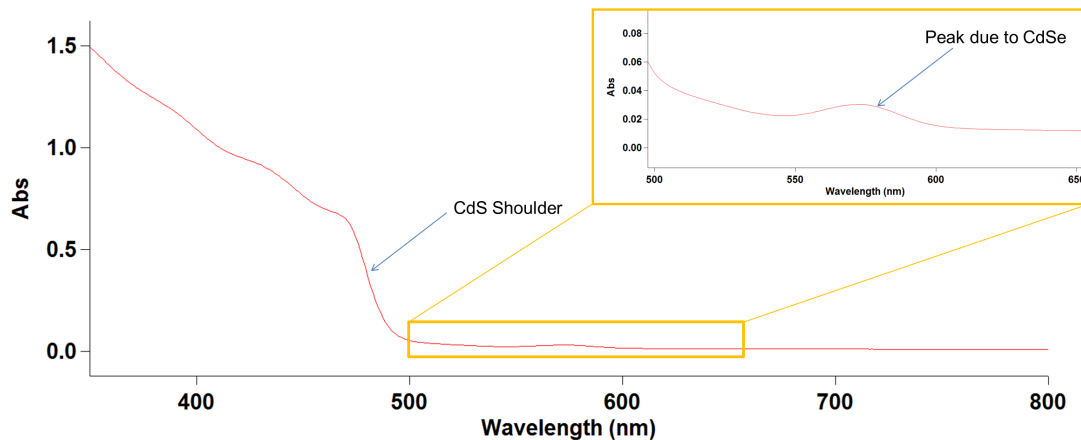


Figure S8. UV-Vis spectrum of plain CdS@CdSe nanorods

- ¹ Amirav, L., Alivisatos A.P., *J. Phys. Chem. Lett.*, **1**, 1051-1054, 2010
- ² Amirav, L., Alivisatos A.P., *J. Am. Chem. Soc.*, **135**, 13049-13053, 2013
- ³ G. Menagen, J.E. Macdonald, Y. Shemesh, I. Popov, U. Banin, *J. Am. Chem. Soc.*, **131**, 17406-17411, 2009
- ⁴ Yu, W. W.; Peng, X. G., *Angew. Chem. Int. Ed.* **2002**, 41 (13), 2368–2371.
- ⁵ Yu, W. W.; Qu, L. H.; Guo, W. Z.; Peng, X. G., *Chem. Mater.* **2003**, 15 (14), 2854–2860.
- ⁶ Iwase, A., Kato, H., Kudo, A., *Chem Soc. Jap.*, **34**, 946-947, 2005
- ⁷ Liu, Y., Masumoto, H., Goto, T., *Mat. Tran.*, **2004**, 45, 900-903
- ⁸ Rubel, M., Haasch, R., Mrozek, P., Wieckowski, A., De Pauli, C., Trasatti, S. *Vacuum*, **1994**, 45(4), 423–427
- ⁹ Shukla, A. K., Kannan, A. M., Hegde, M. S., & Gopalakrishnan, J. *Journal of Power Sources*, **1991**, 35(2), 163–173
- ¹⁰ Peuckert, M., *Surface Science*, **1984**, 144(2–3), 451–464.
- ¹¹ Hammond, C., Schümperli, M. T., Conrad, S. & Hermans, I. *ChemCatChem* **2013**, 5, 2983–2990
- ¹² Banerjee, W., Maikap, S., Lai, C.-S., Chen, Y.-Y., Tien, T.-C., Lee, H.-Y., et al. *Nanoscale Research Letters*, **2012**, 7(1), 1–12
- ¹³ Ryu, W.-H., Lee, Y. W., Nam, Y. S., Youn, D.-Y., Park, C. B., Kim, I.-D. *Journal of Materials Chemistry A*, **2014**, 2(16), 5610–5615
- ¹⁴ ThermoScientific XPS - XPS Interpretation of oxygen <http://xpssimplified.com/elements/oxygen.php> (accessed Sept 6, 2014)
- ¹⁵ W. Mokwa, B. Wessling, and U. Schnakenberg, *Proc. 29th Ann. Int. IEEE EMBS Conf., Lyon, France*, **2007**, pp. 6047–6050
- ¹⁶ Miao, M.S. & Seshadri, R., *J. of Phy.: Cond. Mat.*, **2012**, 24 (21), 215503